Scientific Research Publishing

Open Journal of Biophysics, 2022, 12, 223-233
https://www.scirp.org/journal/ojbiphy
ISSN Online: 2164-5396
ISSN Print: 2164-5388

ISFET Based Immunosensor

Ferdinand Gasparyan[1,2], Lusine Gasparyan[2], Vahan Simonyan[2]

[1]Yerevan State University, Yerevan, Armenia
[2]DNA-HIVE LLC, Rockville, MD, USA
Email: fgaspar@ysu.am

How to cite this paper: Gasparyan, F., Gasparyan, L. and Simonyan, V. (2022) ISFET Based Immunosensor. *Open Journal of Biophysics*, **12**, 223-233.
https://doi.org/10.4236/ojbiphy.2022.124010

Received: September 17, 2022
Accepted: October 22, 2022
Published: October 25, 2022

Abstract

A new design of an immunosensor for viral molecules based on the ISFET nanoscale structure has been proposed. Physical processes take place inimmunosensor are modeled. The effect of modulation of the surface potential of the interface between a semiconductor depleted layer (channel) and a dielectric during the interaction and immobilization of viral molecules was used. Analytical expression for the source-drain current of ISFET as a function of virus types and concentration is presented and analyzed. Dependency of the source-drain current vs. concentration of viruses is analyzed for the COVID-19 virus.

Keywords

Biosensor, ISFET, Antibody, Virus, Sensitivity

1. Introduction

The threat to global health from viral infections, such as COVID-19, influenza, HIV, hepatitis, Zika, Ebola, etc., has brought into sharp focus the need for rapid, sensitive and selective detection of viruses as well as post-infection antibodies. To solve this problem, devices based on field-effect transistors (FETs) are widely used. In the field of chemical and bio-sensorics, ion-selective field-effect transistors (ISFETs) are used. Invented in 1970 by Piet Bergveld, the ISFET was the first FET based biosensor (BioFET) [1]. The ISFET has now become the basic building block of modern sensor technology [2]. In recent years there has been great progress in applying FET-type biosensors for highly sensitive biological detection. Among them, the ISFET and its latest architectures are the most intriguing approaches in electrical biosensor technology [3].

The electrical sensitivity of the ISFET is totally controlled by the properties of electrolyte, oxide, semiconductor and oxide-electrolyte interface state. Much at-

tention is being paid to the development of semiconductor-based biosensors due to the many advantages they offer, including high sensitivity, faster response times, miniaturization, and low cost manufacturing for rapid biospecific analysis with reusable features. Many devices have been developed for monitoring biological processes, such as nucleic acid hybridization, protein-protein interaction, antigen-antibody bonds, DNA-gold electrode nucleotide bonds, substrate-enzyme reactions, etc.

The Immunologically sensitive FETs (ImFETs) represent the amalgamation of the technologies of solid-state electronics and immunodiagnostics. The immunosensors are fabricated by immobilizing immunoagent, preferably, antibody on the gate region of an ISFET. The unique ISFET transduction mechanism could, in principle, be made possible for detection of a wide array of analytes, ranging from small biomolecules to bacteria. There have been several studies describing the application of ISFET as the ImFET [4]. ImFETs have been developed for the detection and quantification of β-bungarotoxin (β-BuTx) [5], the 85 B antigen complex (Ag85B) [6], and for the detection of the TNF-α protein [7]. Also known biosensors based on nanostructures [8] [9] [10] [11] an extended gate FET (EGFET) [12] [13], and organic electrochemical transistors (OECTs) [14].

Some electrophysical properties of BioFET sensors have also been studied in detail by us [15] [16].

A detailed analysis of the experimental and theoretical works devoted to the study of the various types of ISFET-based immunosensors showed:

- ✓ There are no detailed analytical studies of electrophysical and kinetic processes occurring in the solid part (semiconductor, insulator/oxide), aqueous solution and interfaces (electrolyte-insulator, insulator-semiconductor) of ISFET-based biosensors of various architectures. Accordingly, no specific analytical formulas are proposed that describe the dependence of the signal current on the electrical and geometric parameters of the semiconductor, the oxide layer (layers), the number of foreign particles and molecules in aqueous solution and the state of the interfaces.
- ✓ There are no analytical dependences on the type, charge state, size and concentration of analytes or viruses in aqueous solution.

The purpose of this article is to theoretically model and analyze the physical processes occurring in ISFET-based immunosensors, determine the dependence of the source-drain current on the type and concentration of the unknown viruses in an aqueous solution, analyze the sensitivity of such sensors to the presence of various viruses, propose new solutions, new opportunities and expand areas of application of ISFET-based immunosensors.

2. Physical Processes in the ISFET Based Immunosensors

To study the source-drain current (as an information signal) of the ISFET immunosensor and its sensitivity to the presence of foreign molecules and various viruses in an aqueous solution, it is necessary to consider the physical processes

occurring, in particular, at the interface between the gate insulator of the ISFET and the aqueous solution. It is clear that it is on this interface that antibodies and the corresponding virus molecules associated with them will be immobilized. The main design and physical processes taking place in the ISFET immunosensor for molecules and viruses detection are sketched in **Figure 1**. It is presented a schematic representation of proposed ISFET-based immunosensor (a), one separate sensitive "line" (array) in the form of ISFET line, distribution of the applied gatepotential V_g over the layered structure (b), and energetic band diagram picture of the electrolyte-insulator-semiconductor (EIS) structure (c). Particularly silicon based structures and silicon dioxide as a insulator will be discussed. In **Figure 1** RE is the reference electrode, V_g is the applied gate voltage, φ_{Si}, φ_{ch}, φ_{ox}, φ_{Ab}, φ_V and φ_{dl} are potentials on the silicon substrate, current channel (semiconductor depletion layer), oxide layer, antibody layer, virus molecules layer and double layer[1], correspondingly.

The balance equation for the potentials according to **Figure 1** can be represented as:

$$V_g = \varphi_{Si} + \varphi_{ch} + \varphi_{ox} + \varphi_{cl}. \tag{1}$$

To estimate these potentials as well as the threshold voltage, V_{th}, and flat-band voltage, V_{FB}, we can use the following relations [17] [18] [19] [20] [21]:

$$\begin{aligned}
&V_{th} = V_{FB} + 2\varphi_F + \varphi_{ch}, V_{FB} = \varphi_{bs} - \varphi_{ch} + \varphi_{cl} + \varphi_{ox} - \frac{\Phi_{Si} - \Phi_{ox}}{e},\\
&\varphi_{cl} = \varphi_{dl} + \varphi_{Ab} + \varphi_V, \varphi_{bs} \approx 0, \varphi_{Si} \approx 0, \varphi_F = 2\varphi_T \ln\frac{N_A}{n_i},\\
&\varphi_{ch} = \sqrt{\frac{4e\varepsilon_0\varepsilon_{Si}N_A\varphi_T}{C_{ox}^2}}, \varphi_T = \frac{k_BT}{e}, \varphi_{dl} = 2\varphi_T\left(\frac{\varepsilon_w}{\varepsilon_r}\frac{N_{sol}}{K_{AK}^+ + H_s^+}\right),\\
&\varphi_{ox} = \frac{Q_{ox}}{C_{ox}} = \frac{eN_td_{ox}}{\varepsilon\varepsilon_{ox}}, \varphi_{Ab} = \frac{eN_{Ab}d_{Ab}}{\varepsilon_0\varepsilon_{Ab}}, \varphi_V = \frac{eN_Vd_V}{\varepsilon_0\varepsilon_V}.
\end{aligned} \tag{2}$$

In the above expressions e is the elementary charge, k_B is the Boltzmann's constant, T is the absolute temperature, φ_T is the thermal voltage, φ_F is the Fermi potential, φ_{bs} and φ_{Si} are the electric potentials of the bulk solution and the bulk silicon substrate (they usually have very low values, and in what follows we take them as zero), φ_{dl}, φ_{Ab} and φ_V are the potential drop on the double layer, layers of antibody and virus molecules, correspondingly, Φ_{Si} and Φ_{ox} are the work functions of silicon and silicon dioxide (SiO_2), Q_{ox} is the oxide layer charge per unit area, C_{ox} is the capacitances of the oxide layer per unit area, ε_0, ε_{Si}, ε_{ox}, ε_w, ε_r, ε_{Ab} and ε_V are the dielectric permittivity

[1]A double layer is a structure that appears on the surface of a SiO_2 when it is exposed to an aqueous solution. The double layer refers to two parallel layers of charge surrounding the SiO_2. The first layer, the surface charge (either positive or negative), consists of ions adsorbed onto the SiO_2 due to chemical interactions. The second layer is composed of ions attracted to the surface charge via the Coulomb force, electrically screening the first layer. This second layer is loosely associated with the SiO_2. It is made of free ions that move in the aqueous solution under the influence of electric attraction and thermal motion rather than being firmly anchored. It is thus called the "diffuse layer".

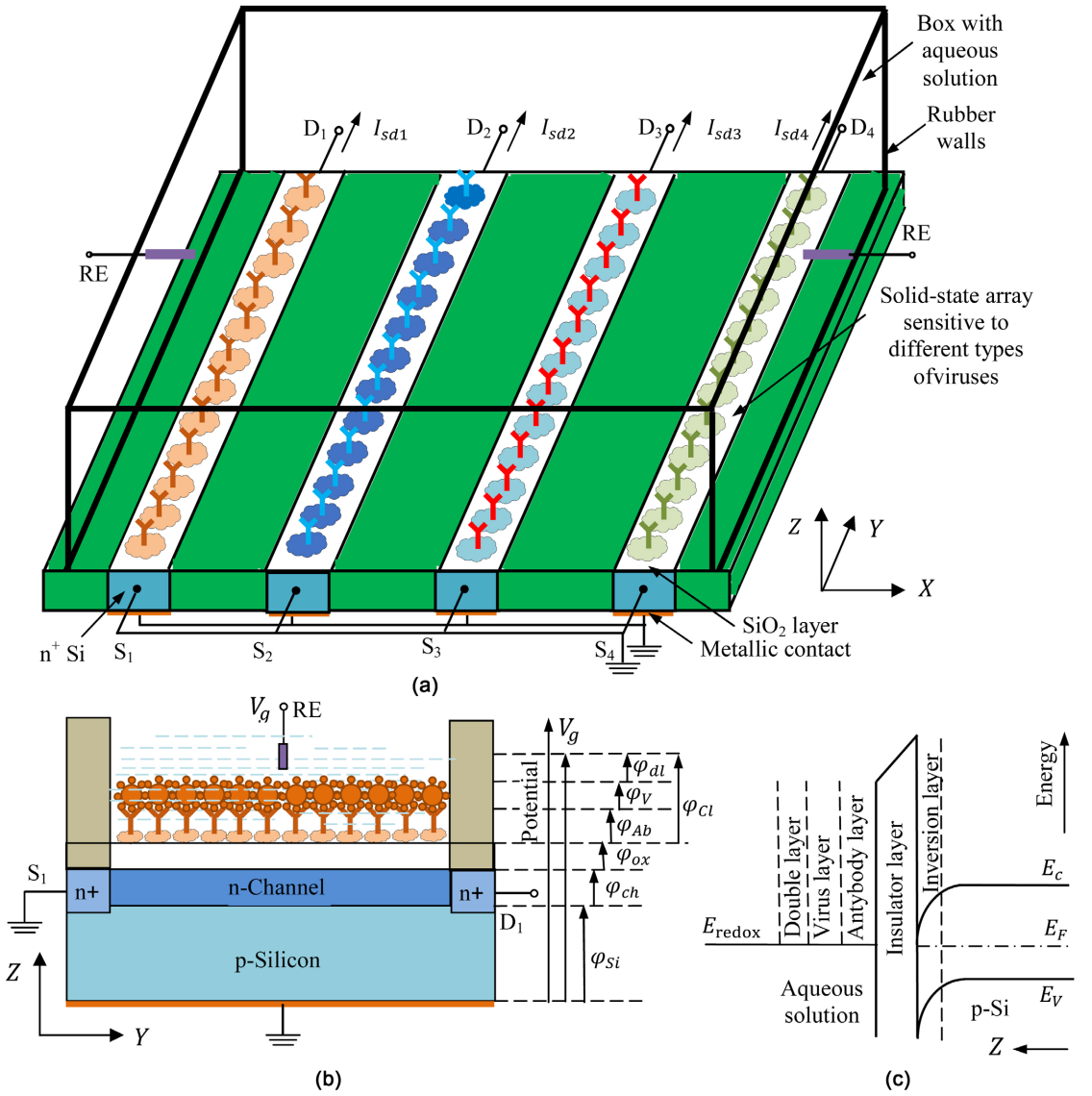

Figure 1. (a) Schematic picture of proposed ISFET based immunosensor for identification and characterization of 4 different viruses and the coordinate system to use. (b) One separate sensitive line (array) and distribution of the applied gate voltage V_g. (c) Energetic band diagram picture of the structure under study. S_1-S_4 and D_1-D_4 are source and drain electrodes, correspondingly, I_{sd1}-I_{sd4} are source-drain currents from 4 separate arrays, correspondingly, E_c, E_V and E_F are conductance, valence and Fermi equilibrium energy levels, correspondingly.

of free space, Si, SiO_2, water, electrolyte, antibody and viruses, respectively, N_A is the doping acceptor concentration in p-Si substrate, n_i is the intrinsic carrier concentration in bulk Si, K_{AK}^{+} is the molar concentration of the cations in the aqueous solution, H_s^{+} is the molar concentration of the hydrogen ions at the oxide surface, N_{sol} is the molar concentration of the aqueous solution, N_t, N_{Ab} and N_V are the concentrations of free electronic bonds (traps), antibody and virus molecules on a unit surface area of the oxide layer, correspondingly, d_{ox}, d_{Ab} and d_V are thicknesses of the oxide and antibody layers, and virus diameter, correspondingly. The redox potential E_{redox} is a measure of the ease with which a molecule accepts electrons, and the double layer in solution con-

sists of Inner Helmholtz layer (IHL), Outer Helmholtz layer (OHL) and Gouy-Chapman layer (GCL) [22].

The main physical processes occur in the conductive inversionn-channel. Therefore, for further calculations, it is necessary to determine the surface potential of the interface between the semiconductor depletion layer (channel) and insulator φ_{ch}. It can be calculated using the method proposed in [23]. For the channel surface potential we have following expression:

$$\varphi_{ch} = \varphi_T \ln\left(\frac{\eta C_{ox}\varphi_T N_A}{etn_i^2}\right) + \varphi_T \ln\left\{\ln\left[1+\frac{1}{2}\exp\left(\frac{V_g - V_{th}}{\eta\varphi_T}\right)\right]\right\}. \tag{3}$$

Here

$$\eta = 1 + \frac{C_d}{C_{ox}} \approx 1 + \sqrt{\frac{q\varepsilon_0\varepsilon_{Si}N_A}{2\varphi_T C_{ox}^2}}$$

is the factor of the field-effect transistor non-ideality (C_d is the capacitance of the silicon depletion layer per unit area, **Figure 1**).

3. Source-Drain Current

We consider the case of an inversion n-channel liquid-gated FET (**Figure 1(c)**). It is clear that the majority of processes in the structure are therefore determined by the electrons. The channel source-drain current consists of drift and diffusion components. It is well known that the diffusion component is dominant in the sub-threshold mode and the drift component is dominant in the over-threshold region. The channel source-drain current in Y direction $I_{sd}(y)$ can be calculated using the method of calculating the source-drain current proposed in [23]. For simplicity assuming $\eta \approx 1$ and taking account that oxide layer capacitance for unit area

$$C_{ox} = \frac{\varepsilon_0\varepsilon_{ox}}{d_{ox}}, \tag{4}$$

and applying the results of [23] to our case, the current can be represented as follows:

$$I_{sd}(V_{ds}) \approx qwn_0V_{sd}\frac{t}{l}\left[\mu_0 - \theta\left(V_g + V_{th}\right)\right]\left\{1+\frac{l_s}{t}\left\{\frac{et^2n_i^2}{\varepsilon_0\varepsilon_{ox}\varphi_T N_A} + \ln\left(\frac{\varphi_T\varepsilon_0\varepsilon_{ox}N_A}{qt^2n_i^2}\right) + \ln\left[\ln\left(1+\frac{1}{2}\exp\left(\frac{V_g+V_{th}}{\varphi_T}\right)\right)\right]\right\}\left(1-\mathrm{e}^{-t/l_s}\right)\right\} \tag{5}$$

Here

$$l_s = \frac{L_D}{1+p_0/n_0}, \quad L_D = \sqrt{\frac{\varepsilon_0\varepsilon_{Si}\varphi_T}{qn_0}}, \tag{6}$$

V_{sd} is the source-drain voltage, w, l and t are the inversion channel width, length and thickness, correspondingly, L_D is the Debye screening length, n_0 and p_0 are the concentrations of the equilibrium electrons and holes. The

electron's mobility dependence on the transversal electric field (Y direction) at the applied gate voltage was taken into account using the following empiric equation [24]:

$$\left(\mu_{ef}\right)_x = \mu_0 - \theta\left(V_{th} + V_g\right), \tag{7}$$

where μ_0 is the low-field magnitude of the mobility, θ is the coefficient taken as 28 cm^2/(Vs) [24] [25].

The electrical field in the inversion layer of the semiconductor caused by the applied gate voltage changes the transport behavior of the charge carriers and results in more frequent scattering events than in the absence of the gate voltage. Since the modeling and the measurements are performed for low drain biases in linear mode, the effect of the electron velocity saturation on the drain current can be neglected.

The dependence of the source-drain current of the transistor on the types, geometric dimensions and concentration of viruses can be determined through expressions φ_{Ab} and φ_V.

For simplicity, in numerical calculations we will assume that the concentrations of immobilized antibodies and viruses in the aqueous solution are the same ($N_{Ab} = N_V$). Then dependency of source-drain current from virus types, sizes and concentration will be determined by the ε_V, d_V and N_V.

Numerical Simulation and Discussion for the Case of Covid-19 Virus

For the numerical analysis, below we used the parameters of the Covid-19 virus. To date, research has shown that the viruses that have been identified and isolated can range in diameter size from 20 nm to as large as 500 nm. Aside from spherical virus particles like SARS-CoV-2, whose diameters provide information on their sizes, the length of rod- or filament-shaped viruses can measure to as long as 1000 nm [26]. Measured value of dielectric constant varies from 35 - 65 in the frequency range up to 12 GHz [27], For SARS-CoV-2 the average dielectric constant on the protein-water interface is about 20 - 30 [28], the average size of the spike protein is 10 to 20 nm, and the feature height of particles after BSA (Bovine Serum Albumin) blocking is 4.59 ± 1.75 nm [28]. The height of protein particles is increased to 8.17 ± 1.77 nm, verifying the binding of antibody with antigen. The height of antigen and antibody complex is around 6.3 nm.

Some known electrophysical parameters of the silicon substrate, silicon dioxide and aqueous solution we use from [20] [23]. They are:

$w = 0.5$ cm; $t = 5\times10^{-3}$ cm; $l = 1$ cm; $d_{Ab} = 2\times10^{-5}$ cm; $d_V = 3\times10^{-5}$ cm;
$d_{ox} = 4\times10^{-6}$ cm; $\mu_0 = 1400$ cm^2/V·s; $\theta = 28$ cm^2/V·s; $\varphi_T = 0.026$ V;
$\Phi_{Si} = 4.8$ eV; $\Phi_{ox} = 5$ eV; $N_A = 10^{15}$ cm^{-3}; $n_0 = 10^{15}$ cm^{-3}; $p_0 = 2.25\times10^5$ cm^{-3};
$n_i = 1.5\times10^{10}$ cm^{-3}; $N_t = 10^{11}$ cm^{-2}; $N_{sol} = 0.015$ mol/l; $K_{AK}^{+} = 0.001$ mol/l;
$H_s^{+} = 0.005$ mol/l; $N_{Ab} = 10^7$; $\varepsilon_0 = 8.85\times10^{-14}$ F/cm; $\varepsilon_w = 80$; $\varepsilon_r = 78$;
$\varepsilon_{Ab} = 50$; $\varepsilon_V = 25$; $\varepsilon_{ox} = 3.8$; $\varepsilon_{Si} = 11.7$.

In Figure 2 presented dependencies $I_{sd}(V_{sd})$ for the several values of virus concentration at the $V_g = 1\,\text{V}$. The source-drain current increases linearly with the source-drain voltage and with increasing virus concentration (Figure 2). At a relatively low concentration of viruses, the source-drain current practically do not change. At concentrations of the order of $N_V \propto 10^3 \div 10^4\,\text{cm}^{-2}$, I_{sd} changes slowly (see Figure 3) and increases more rapidly as the concentration rises above $10^5\,\text{cm}^{-2}$. It is clear that there is some threshold value of the virus molecules concentration in order of $10^2 \div 10^3\,\text{cm}^{-2}$.

The sensitivity S of the source-drain current vs. virus molecules concentration slowly increase beginning of the threshold concentration and can determine as follows:

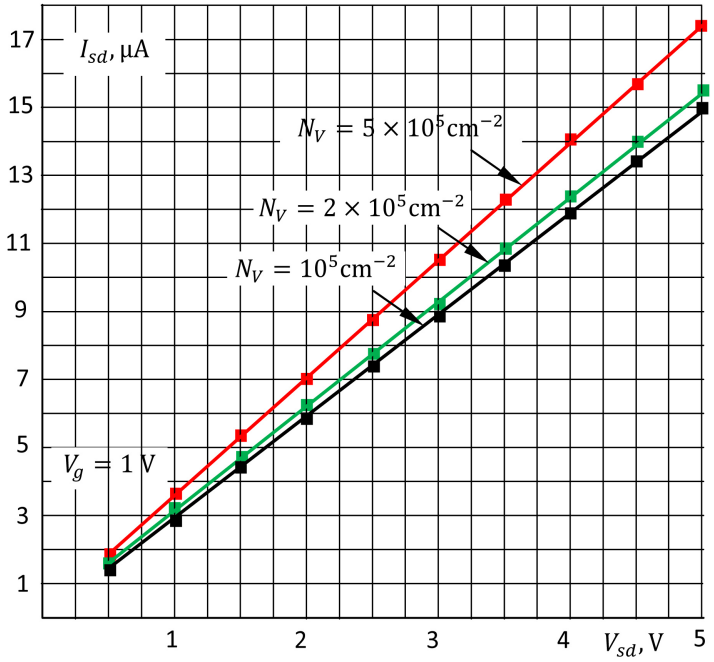

Figure 2. Dependency of source-drain current vs. source-drain voltage at the $V_g = 1\,\text{V}$.

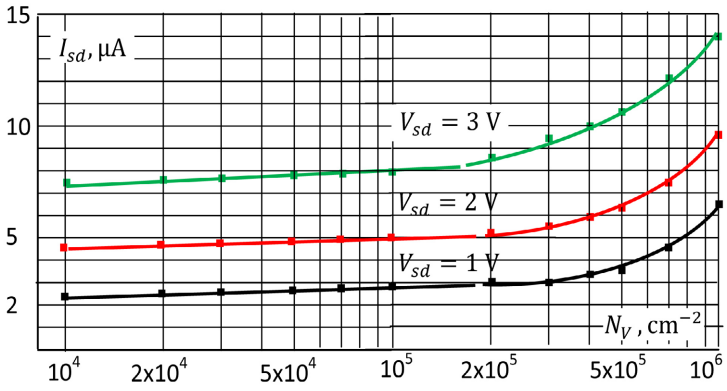

Figure 3. Dependency of source-drain current vs. virus molecules concentration N_V at the $V_g = 1\,\text{V}$.

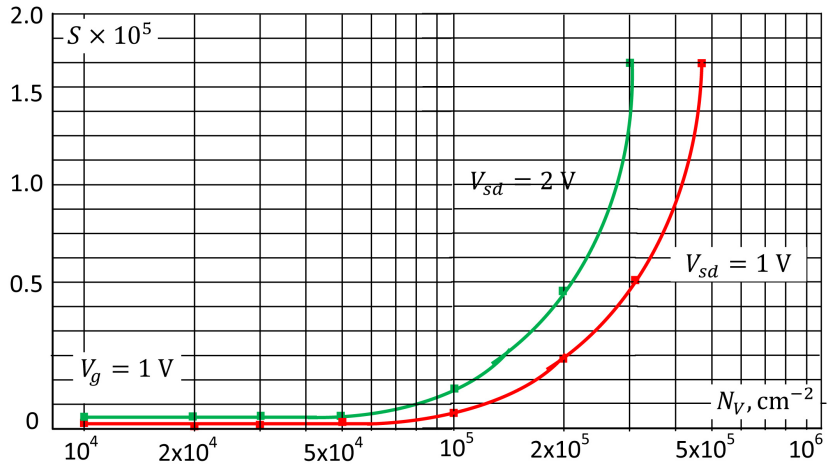

Figure 4. Dependency of current sensitivity vs. virus molecules concentration N_V at the $V_g = 1$ V.

$$S = \frac{\Delta I_{sd}}{\Delta N_V}.$$

Here ΔI_{ds} and ΔN_V are the elementary increments in the source-drain current and virus molecules concentration, accordingly.

Dependency of current sensitivity vs. virus molecules quantity N_V presented in **Figure 4**.

For repeated use of the proposed construction, it is necessary to purify antibodies from viruses bound to them. Affinity chromatography is an efficient antibody, antigen and protein separation method based on the interaction between specific immobilized ligands and target antibody, antigen, and so on. Populations of available ligands can be used to separate antibodies or their Fab fragments. The detail of repeated use presented in [29] [30].

4. Conclusions

Based on the theoretical modeling of the operation of the ISFET immunosensor and the obtained dependencies for the COVID-19 virus, the following important conclusions can be drawn:

1) Unknown virus detection

With known or given values of gate and source-drain (V_g and V_{sd}) voltages by the change of magnitude of the measured source-drain current I_{sd}, it is possible to detect the presence of foreign unknown molecules and viruses in the aqueous solution.

2) Unknown virus identification

With known or given values of gate and source-drain (V_g and V_{sd}) voltages by the magnitude of the measured source-drain current I_{sd}, it is possible to determine the type of unknown viruses.

3) Unknown virus concentration definition

With known or given gate and source-drain (V_g and V_{sd}) voltages by the

magnitude of the measured source-drain current I_{sd}, it is possible to determine the concentration of unknown viruses in the range 10^4 - 10^6 cm^{-2}.

4) Detection sensitivity for unknown virus

By selecting the gate and source-drain (V_g and V_{sd}) voltages the sensitivity of the ISFET immunosensor can be adjusted to detect unknown viruses.

Author Contribution Information

All authors participated in the statement of the problem and discussion of the results. L. Gasparyan, and F. Gasparyan conducted literature review. F. Gasparyan and V. Simonyan made calculations and participated in the writing of the text of the article.

Conflicts of Interest

The authors declare no conflicts of interest regarding the publication of this paper.

References

[1] Bergveld, P. (1970) Development of an Ion-Sensitive Solid-State Device for Neurophysiological Measurements. *IEEE Transactions on Biomedical Engineering*, **BME-17**, 70-71. https://doi.org/10.1109/TBME.1970.4502688

[2] Bergveld, P. (1986) The Development and Application of FET-Based Biosensors. *Biosensors*, **2**, 15-33. https://doi.org/10.1016/0265-928X(86)85010-6

[3] Lee, C.-S., Kim, S.K. and Kim, M. (2009) Ion-Sensitive Field-Effect Transistor for Biological Sensing. *Sensors*, **9**, 7111-7131. https://doi.org/10.3390/s90907111

[4] Zachariah, E.S., Gopalakrishnakone, P. and Neuzil, P. (2006) Immunologically Sensitive Field-Effect Transistors. In: Webster, J.G., Ed., *Encyclopedia of Medical Devices and Instrumentation*, John Wiley & Sons, Inc., Hoboken, 98-110. https://doi.org/10.1002/0471732877.emd141

[5] Selvanayagam, Z.E., Neuzil, P., Gopalakrishnakone, P., Sridhar, U., Singh, M. and Ho, L.C. (2002) An ISFET-Based Immunosensor for the Detection of β-Bungarotoxin. *Biosensors and Bioelectronics*, **17**, 821-82. https://doi.org/10.1016/S0956-5663(02)00075-1

[6] Saengdee, P., Chaisriratanakul, W., Bunjongpru, W., *et al*. (2016) A Silicon Nitride ISFET Based Immunosensor for Ag85B Detection of Tuberculosis. *The Analyst*, **141**, 5767-5775. https://doi.org/10.1039/C6AN00568C

[7] Vozgirdaite, D., Halima, H.B., Bellagambi, F.G., *et al*. (2021) Development of an ImmunoFET for Analysis of Tumour Necrosis Factor-α in Artificial Saliva: Application for Heart Failure Monitoring. *Chemosensors*, **9**, Article No. 26. https://doi.org/10.3390/chemosensors9020026

[8] Hosseini, M., Fathollahzadeh, M., Kolahdouz, M., Rostamian, A., Mahmoodian, M., Samaeian, A. and Radamson, H.H. (2018) ISFET Immunosensor Improvement Using Amine-Modified Polystyrene Nanobeads. *Journal of Solid State Electrochemistry*, **22**, 3161-3169. https://doi.org/10.1007/s10008-018-4025-9

[9] Liu, X., Lin, P., Yan, X., *et al*. (2013) Enzyme-Coated Single ZnO Nanowire FET. *Sensors and Actuators B: Chemical*, **176**, 22-27. https://doi.org/10.1016/j.snb.2012.08.043

[10] Fathollahzadeh, M., Hosseini, M., Norouzi, M., *et al*. (2018) Immobilization of Glucose Oxidase on ZnO Nanorods Decorated Electrolyte-Gated Field Effect Transistor for Glucose Detection. *Journal of Solid State Electrochemistry*, **22**, 61-67. https://doi.org/10.1007/s10008-017-3716-y

[11] Anvarifard, M.K., Ramezani, Z. and Amiri, I.S. (2020) Label-Free Detection of DNA by a Dielectric Modulated Armchair-Graphene Nanoribbon FET Based Biosensor in a Dual-Nanogap Setup. *Materials Science and Engineering: C*, **117**, Article ID: 111293. https://doi.org/10.1016/j.msec.2020.111293

[12] Pullano, S.A., Critello, C.D., Mahbub, I., Tasneem, N.T., Shamsir, S., Islam, S.K., Greco, M. and Fiorillo, A.S. (2018) EGFET-Based Sensors for Bioanalytical Applications: A Review. *Sensors*, **18**, Article No. 4042. https://doi.org/10.3390/s18114042

[13] Kamahori, M., Ishige, Y. and Shimoda, M, (2008) Enzyme Immunoassay Using a Reusable Extended-Gate Field-Effect-Transistor Sensor with a Ferrocenylalkanethiol-Modified Gold Electrode. *Analytical Sciences*, **24**, 1073-1079. https://doi.org/10.2116/analsci.24.1073

[14] Marquez, A.V., McEvoy, N. and Pakdel, A. (2020) Organic Electrochemical Transistors (OECTs) toward Flexible and Wearable Bioelectronics. *Molecules*, **25**, Article No. 5288. https://doi.org/10.3390/molecules25225288

[15] Gasparyan, L., Mazo, I., Simonyanand, V. and Gasparyan, F. (2020) Noises and Signal-to-Noise Ratio of Nanosize EIS and ISFET Biosensors. *Open Journal of Biophysics*, **10**, 1-12. https://doi.org/10.4236/ojbiphy.2020.101001 https://www.scirp.org/journal/ojbiphy

[16] Gasparyan, L., Gasparyan, F. and Simonyan, V. (2021) Internal Electrical Noises of BioFET Sensors Based on Various Architectures. *Open Journal of Biophysics*, **11**, 177-204. https://doi.org/10.4236/ojbiphy.2021.112006

[17] Gasparyan, F.V., Poghossian, A., Vitusevich, S.A., Petrychuk, M.V., Sydoruk, V.A., Siqueira, J.R., Oliveira, O.N., Offenhäusser, A. and Schöning, M.J. (2011) Low-Frequency Noise in Field-Effect Devices Functionalized with Dendrimer/Carbon-Nanotube Multilayers. *IEEE Sensors Journal*, **11**, 142-149. https://doi.org/10.1109/JSEN.2010.2052355

[18] Janicki, M., Daniel, M., Szermer, M. and Napieralski, A. (2004) Ion Sensitive Field Effect Transistor Modeling for Multidomain Simulation Purposes. *Microelectronics Journal*, **35**, 831-840. https://doi.org/10.1016/j.mejo.2004.06.015

[19] Hassibi, A., Navid, R., Dutton, R.W. and Lee, T.H. (2004) Comprehensive Study of Noise Processes in Electrode Electrolyte Interfaces. *Journal of Applied Physics*, **96**, 1074-1082. https://doi.org/10.1063/1.1755429

[20] Sze, S.M. and Ng, K.K. (2006) Physics of Semiconductor Devices. 3rd Edition, John Wiley & Sons, Hoboken. https://doi.org/10.1002/0470068329

[21] Ytterdal, T., Cheng, Y. and Fjeldly, T.A. (2003) Device Modeling for Analog and RF CMOS Circuit Design. John Wiley & Sons, Hoboken. https://doi.org/10.1002/0470863803

[22] Nakamura, M., Sato, N., Hoshi, N. and Sakata, O. (2011) Outer Helmholtz Plane of the Electrical Double Layer Formed at the Solid Electrode-Liquide Interface. *ChemPhysChem*, **12**, 1430-1434. https://doi.org/10.1002/cphc.201100011

[23] Pud, S., Gasparyan, F., Petrychuk, M., Li, J., Offenhausser, A. and Vitusevich, S.A. (2014) Single Trap Dynamics in Electrolyte-Gated Si-Nanowire Field Effect Transistors. *Journal of Applied Physics*, **115**, Article ID: 233705. https://doi.org/10.1063/1.4883757

[24] Park, C., Lee, C., Lee, K., Moon, B.-J., Byun, Y.H. and Shur, M. (1991) A Unified Current-Voltage Model for Long-Channel nMOSFETs. *IEEE Transactions on Electron Devices,* **38**, 399-406. https://doi.org/10.1109/16.69923

[25] Gildenblat, G.S. and Huang, C.-L. (1989) Engineering Model Foe Inversion Channel Mobility for 60-300 K Temperature Range. *Electronics Letters*, **25**, 634-636. https://doi.org/10.1049/el:19890430

[26] Cuffari, B. (2021) The Size of SARS-CoV-2 and Its Implications. https://www.news-medical.net/health/The-Size-of-SARS-CoV-2-Compared-to-Other-Things.aspx

[27] Abdulkarim, Y.I., Awl, H.N., Muhammadsharif, F.F., Sidiq, K.R., Saeed, S.R., Karaaslan, M., Huang, S., Luo, H. and Deng, L. (2009) Design and Study of a Coronavirus-Shaped Metamaterial Sensor Stimulated by Electromagnetic Waves for Rapid Diagnosis of Covid-19. arXiv:2009.08862.

[28] Liu, H., Yang, A., Song, J., *et al.* (2021) Ultrafast, Sensitive, and Portable Detection of COVID-19 IgG Using Flexible Organic Electrochemical Transistors. *Science Advances*, **7**, eabg8387. https://doi.org/10.1126/sciadv.abg8387

[29] Sheng, S. and Kong, F. (2012) Separation of Antigens and Antibodies by Immunoaffinity Chromatography. *Pharmaceutical Biology*, **50**, 1038-1044. https://doi.org/10.3109/13880209.2011.653493

[30] Ayyar, B.V., Arora, S., Murphy, C. and O'Kennedy, R. (2012) Affinity Chromatography as a Tool for Antibody Purification. *Methods*, **56**, 116-129. https://doi.org/10.1016/j.ymeth.2011.10.007